Distinct Circuits in Anterior Cingulate Cortex Encode Safety Assessment and Mediate Flexibility of Fear Reactions

Kaibin Wu[1,2,3,4,5,9], Dijia Wang[1,2,3,4,5,9], Yuwei Wang[6,9], Peiwen Tang[1,2,3,4,5,9], Xuan Li[1], Yidi Pan[1], Huizhong W. Tao[7,8], Li I. Zhang[7,8], Feixue Liang[1,2,3,4,5,6,10,*]

Supplementary Figures 1-7

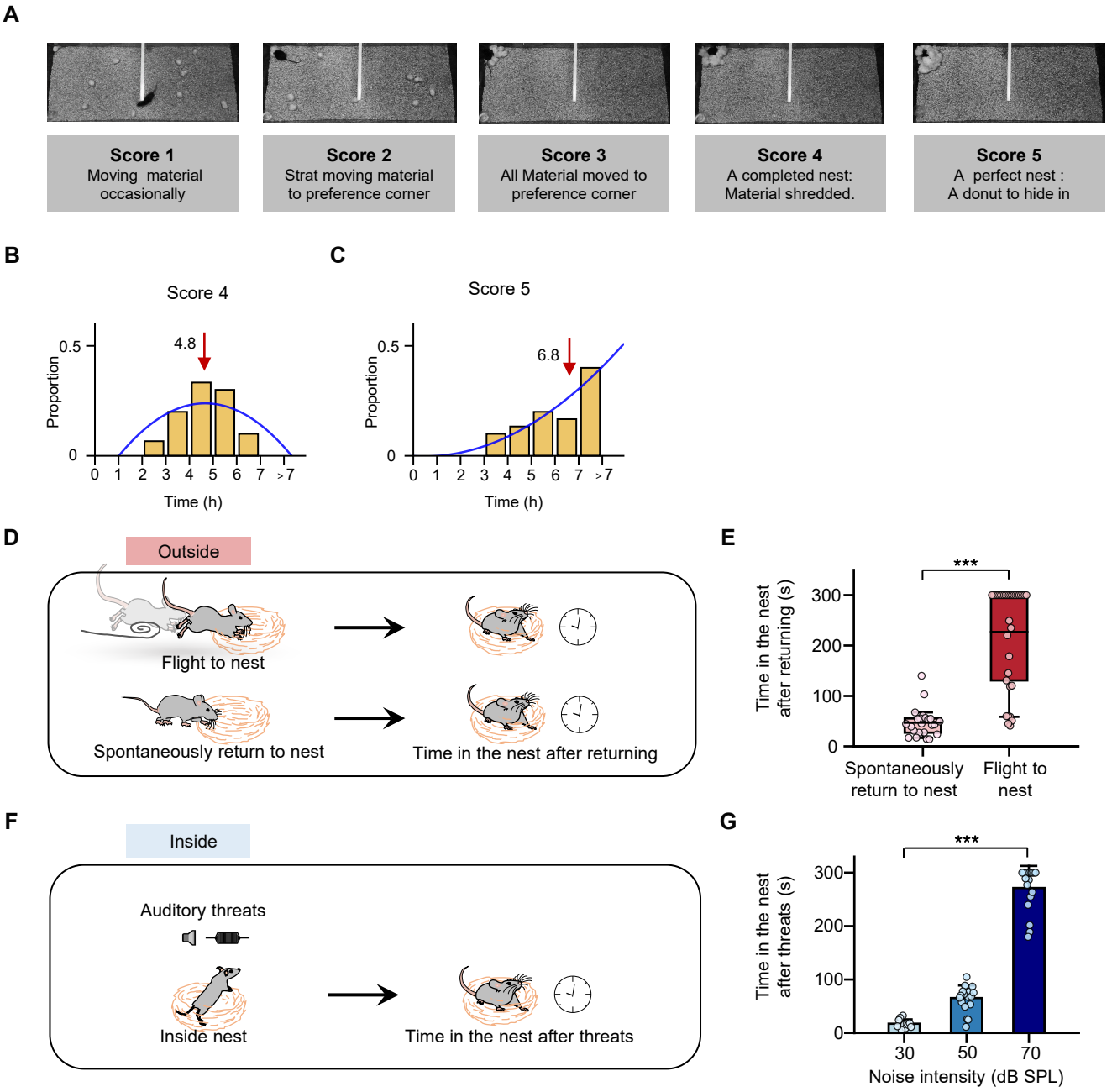

Figure S1. The scoring standards for nest-building and various behavioral parameters. Related to Figure 1.

(**A**) Video frames of nest-building at five typical stages (top) and their scoring standards (bottom).

(**B-C**) Distribution of nest-building times (the time point when a mouse was placed in was hour 0) reaching the score 4 (**B**) or 5 (**C**) stage. Arrow indicates the mean value.

(**D**) Schematic of mice staying inside the self-built nest after threat-triggered returning to the nest.

(**E**) Time spent in the nest after a spontaneous return vs. after threat-triggered return. Mann-Whitney test ($P < 0.001$, $U = 49.00$). n = 23, 34 bouts for spontaneous return and flight, respectively.

(**F**) Schematic of mice remaining in the self-built nest after exposure to auditory threats.

(**G**) Time spent in the nest after experiencing noise sounds at different intensities with the mouse initially inside the self-built nest. Kruskal-Wallis test (***$P < 0.001$, $H = 40.14$), n = 11, 19, 18 trials for 30, 50, 70 dB SPL, respectively.

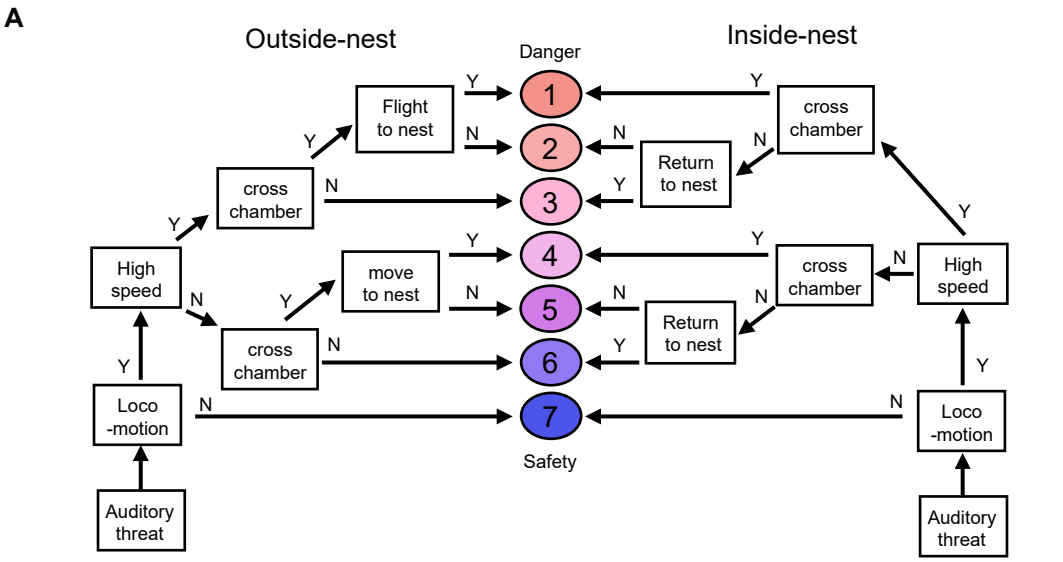
A
Outside-nest
Inside-nest
Danger
Safety
1
2
3
4
5
6
7
Flight to nest
cross chamber
High speed
move to nest
cross chamber
Loco -motion
Auditory threat
Return to nest
cross chamber
High speed
Return to nest
cross chamber
Loco -motion
Auditory threat
Y
N

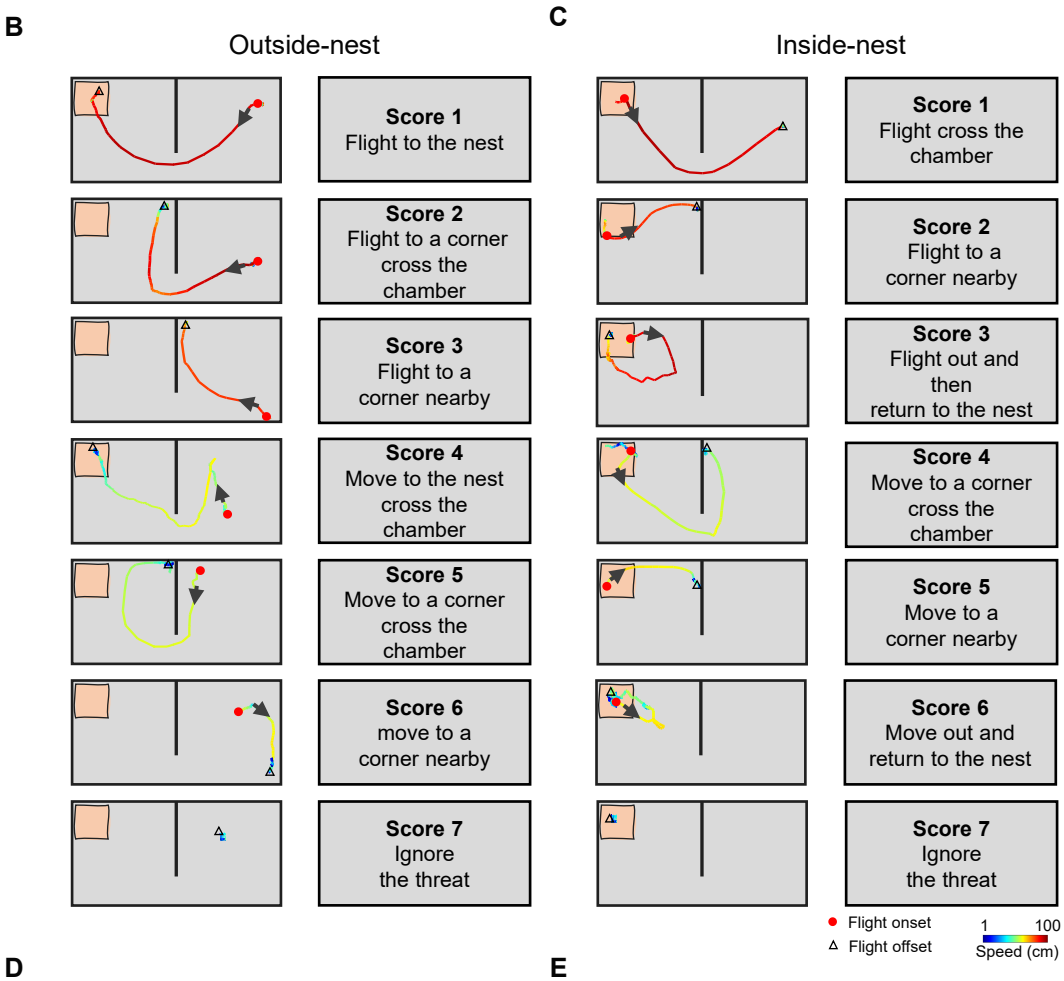
B
Outside-nest
C
Inside-nest
Score 1
Flight to the nest
Score 2
Flight to a corner cross the chamber
Score 3
Flight to a corner nearby
Score 4
Move to the nest cross the chamber
Score 5
Move to a corner cross the chamber
Score 6
move to a corner nearby
Score 7
Ignore the threat
Score 1
Flight cross the chamber
Score 2
Flight to a corner nearby
Score 3
Flight out and then return to the nest
Score 4
Move to a corner cross the chamber
Score 5
Move to a corner nearby
Score 6
Move out and return to the nest
Score 7
Ignore the threat
Flight onset
Flight offset
1
100
Speed (cm)

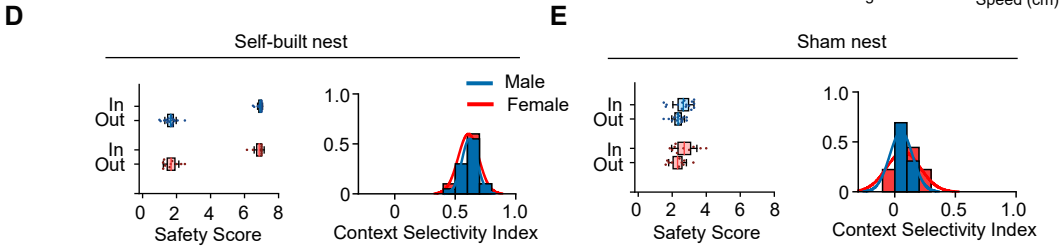
D
Self-built nest
In
Out
In
Out
0
2
4
6
8
Safety Score
Male
Female
1.0
0.5
0
0
0.5
1.0
Context Selectivity Index
E
Sham nest
In
Out
In
Out
0
2
4
6
8
Safety Score
1.0
0.5
0
0
0.5
1.0
Context Selectivity Index

Figure S2. The scoring standards for context-dependent behavioral responses to auditory threats and the behavioral summary for male and female mice. Related to Figure 1.

(**A**) The flow chart for scoring safety/danger-related behaviors both in outside- and inside-nest conditions.

(**B**) Illustration of the standards of safety scores from 1 to 7 in outside-nest bouts.

(**C**) Similar to (B), but for inside-nest bouts.

(**D**) Comparison of safety scores (left) and the distribution of context selectivity indices (CSIs) (right) in different scenarios between male (blue) and female mice (red). Kolmogorov-Smirnov test (P = 0.65, D = 0.25), n = 10 female mice and 20 male mice.

(**E**) Similar to (**D**), but for the sham-nest conditions. Kolmogorov-Smirnov test (P = 0.81, D = 0.33), n = 10 female mice and 15 male mice.

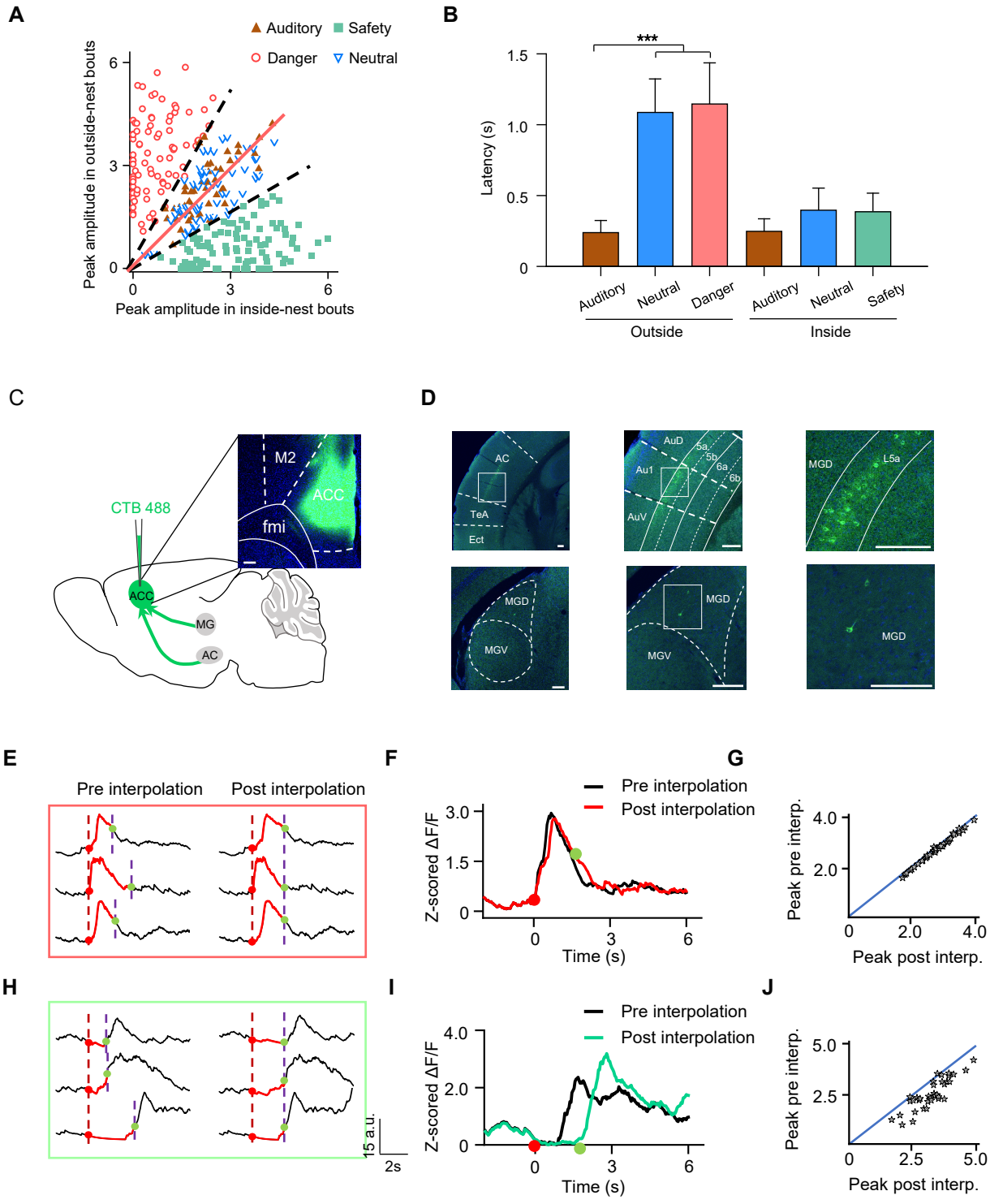
A
Auditory
Safety
Danger
Neutral
Peak amplitude in outside-nest bouts
Peak amplitude in inside-nest bouts
B
***
Latency (s)
Auditory
Neutral
Danger
Auditory
Neutral
Safety
Outside
Inside
C
CTB 488
M2
ACC
fmi
ACC
MG
AC
D
AC
TeA
Ect
AuD
Au1
AuV
6a
6b
MGD
L5a
MGV
E
Pre interpolation
Post interpolation
F
Pre interpolation
Post interpolation
Z-scored ΔF/F
Time (s)
G
Peak pre interp.
Peak post interp.
H
15 a.u.
2s
I
Pre interpolation
Post interpolation
Z-scored ΔF/F
Time (s)
J
Peak pre interp.
Peak post interp.

Figure S3. The analysis of behavioral-event-related neurons. Related to Figure 2 and 3.

(**A**) Peak amplitudes of Ca^{2+} responses of auditory-, danger-, safety-responding neurons and neutral cells in the outside- vs. inside-nest condition. Dashed black lines separate different groups of cells. Red line is the unity line.

(**B**) The average response latency for auditory-, danger-, safety-responding neurons and neutral cells. Kruskal-Wallis test (***$P < 0.001$, $H = 119.75$), $n = 16, 44, 46, 45$ for auditory-, safety-, danger-responding and neutral cells, respectively.

(**C**) Schematic of retrograde tracing of inputs to ACC neurons from the medial geniculate body (MG) and auditory cortex (AC). Inset, example image showing the expression of Alexa Fluor 488-CTB (green) at the injection site.

(**D**) Confocal images showing retrogradely labeled cells in AC and MG with zoom-in images of the boxed areas (right). Scale bar, 100 μm.

(**E**) Example interpolation for a danger-responding neuron. The Ca^{2+} signal trace in the window from the onset of flight (marked by the red dashed line) to the timing of nest-entering (marked by the purple dashed line) of each trial (left panel) was interpolated into a 2 sec long waveform (right panel), and the rest of the waveform was unchanged.

(**F**) Comparison of average traces of pre- and post-interpolation for the cell shown in (**E**).

(**G**) Comparison of peak amplitudes of the average Ca^{2+} signal waveform during 0-2 sec after the flight onset between pre- and post-interpolation. Blue line is the unity line.

(**H**-**J**) Similar to (**E**-**G**), but for a safety-responding cell. Note that after interpolation, the peak amplitude of the average waveform became larger because of a better temporal alignment.

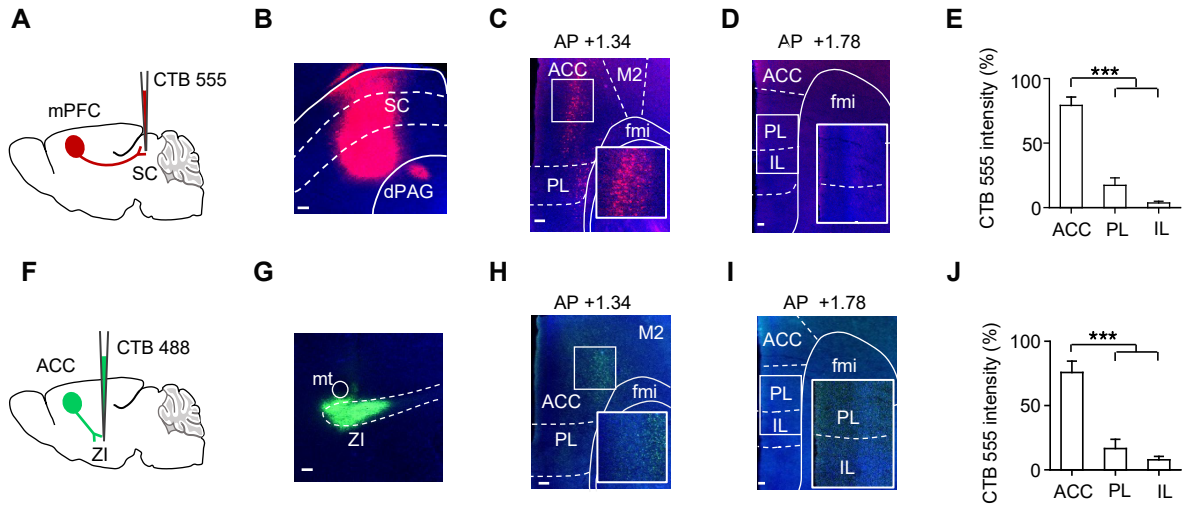

Figure S4. SC- and ZI-projecting neurons in mPFC. Related to figure 4.

(**A**) Schematic of retrograde labeling of SC-projecting neurons in mPFC.

(**B**) CTB 555 fluorescence at the injection site of SC. Scale bar, 100 μm.

(**C**-**D**) Retrogradely labeled SC-projecting neurons in the center section of ACC (AP +1.34 mm) (**C**), PL and IL (AP +1.78 mm) (**D**), respectively. Inset, zoom-in image of the boxed area. Blue, DAPI staining. Scale bar, 100 μm.

(**E**) Relative intensity of CTB labeling in ACC, PL and IL. Kruskal-Wallis test (***P < 0.001, H = 23.14), n = 9 brain slices from 3 mice.

(**F**-**J**) similar to (**A**-**E**), but for ZI-projecting neurons labeled by CTB 488. Kruskal-Wallis test (***P < 0.001, H = 20.43), n = 9 brain slices from 3 mice.

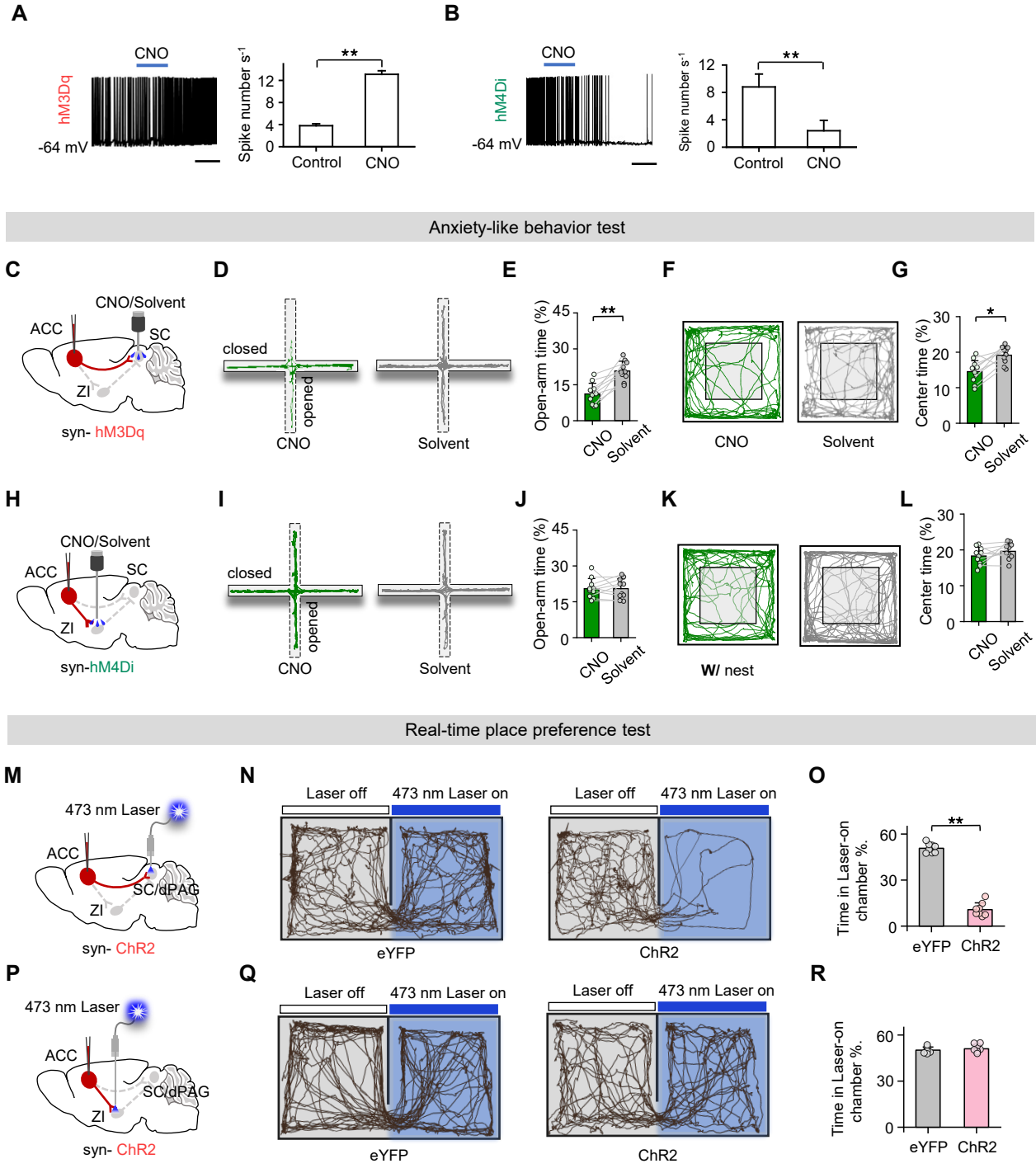
A
CNO
hM3Dq
-64 mV
Spike number s-1
12
8
4
0
**
Control
CNO
B
CNO
hM4Di
-64 mV
Spike number s-1
12
8
4
0
**
Control
CNO
Anxiety-like behavior test
C
CNO/Solvent
ACC
SC
ZI
syn- hM3Dq
D
closed
opened
CNO
Solvent
E
Open-arm time (%)
45
30
15
0
**
CNO
Solvent
F
CNO
Solvent
G
Center time (%)
30
20
10
0
*
CNO
Solvent
H
CNO/Solvent
ACC
SC
ZI
syn-hM4Di
I
closed
opened
CNO
Solvent
J
Open-arm time (%)
45
30
15
0
CNO
Solvent
K
W/ nest
L
Center time (%)
30
20
10
0
CNO
Solvent
Real-time place preference test
M
473 nm Laser
ACC
SC/dPAG
ZI
syn- ChR2
N
Laser off
473 nm Laser on
eYFP
Laser off
473 nm Laser on
ChR2
O
Time in Laser-on chamber %.
60
30
0
**
eYFP
ChR2
P
473 nm Laser
ACC
SC/dPAG
ZI
syn- ChR2
Q
Laser off
473 nm Laser on
eYFP
Laser off
473 nm Laser on
ChR2
R
Time in Laser-on chamber %.
60
30
0
eYFP
ChR2

Figure S5. Validation of the efficacy of chemo/optogenetic manipulations and associated behavioral side effects. Related to figure 6.

(**A**) Left, raw recorded trace showing an increase of firing rate in a hM3Dq-expessing ACC neuron after CNO application. Whole-cell current-clamp recording was performed in the slice preparation. Right, average firing rates before and after perfusion of CNO. Temporal scale, 3 min. Wilcoxon signed rank test (**P = 0.004, W = 45.00), n = 9 brain slices from 3 mice.

(**B**) Similar to (**A**), but for verifying the effectiveness of CNO application in suppressing hM4Di-expessing neurons in ACC. Wilcoxon signed rank test (**P = 0.004, W = 45.00), n = 9 brain slices from 3 mice.

(**C**) Schematic of chemogenetic activation of ACC axon terminals in the SC.

(**D**) Movement tracks of an example mouse in the EPM test with (left) and without (right) chemogenetic activation.

(**E**) Percentage of time spent in open arms of EPM. Two-tailed Wilcoxon matched-pairs signed rank test (CNO vs. Solvent: **P = 0.002, W = 55.00, n = 10 mice each for CNO and Solvent groups).

(**F**) Movement tracks of an example mouse in the OF test.

(**G**) Percentage of time spent in the center of OF. Two-tailed Wilcoxon matched-pairs signed rank test (CNO vs. Solvent: *P = 0.014, W = 51.00, n = 10 mice each for CNO and Solvent groups).

(**H-L**) Similar to (**C**-**G**), but for chemogenetic inhibition of ACC axon terminals in ZI. (**J**) Two-tailed Wilcoxon matched-pairs signed rank test (CNO vs. Solvent: P = 0.63, W = 22.00, n = 10 mice each for CNO and Solvent).

(**L**) Two-tailed Wilcoxon matched-pairs signed rank test (CNO vs. Solvent: P = 0.23, W = 15.00, n = 10 mice each for CNO and Solvent).

(**M**) Schematic of optogenetic activation of ACC axon terminals in the SC/dPAG.

(**N**) Locomotion tracking for an example animal in the eYFP control or ChR2 group during a 10-min session of RTPP test with optogenetic activation of ACC glutamatergic axon terminals in SC/dPAG.

(**O**) Comparison of percentage time spent in the laser-on chamber between the eYFP (n = 8 mice) and ChR2 (n = 8 mice) groups. Wilcoxon signed rank test (**P = 0.003, W= 36.00).

(**P-R**) Similar to (**M**-**O**), but for optogenetic activation of ACC glutamatergic axon terminals in ZI. Wilcoxon signed rank test (P = 0.56, W = 28.00, n = 7 mice for both eYFP and ChR2 groups).

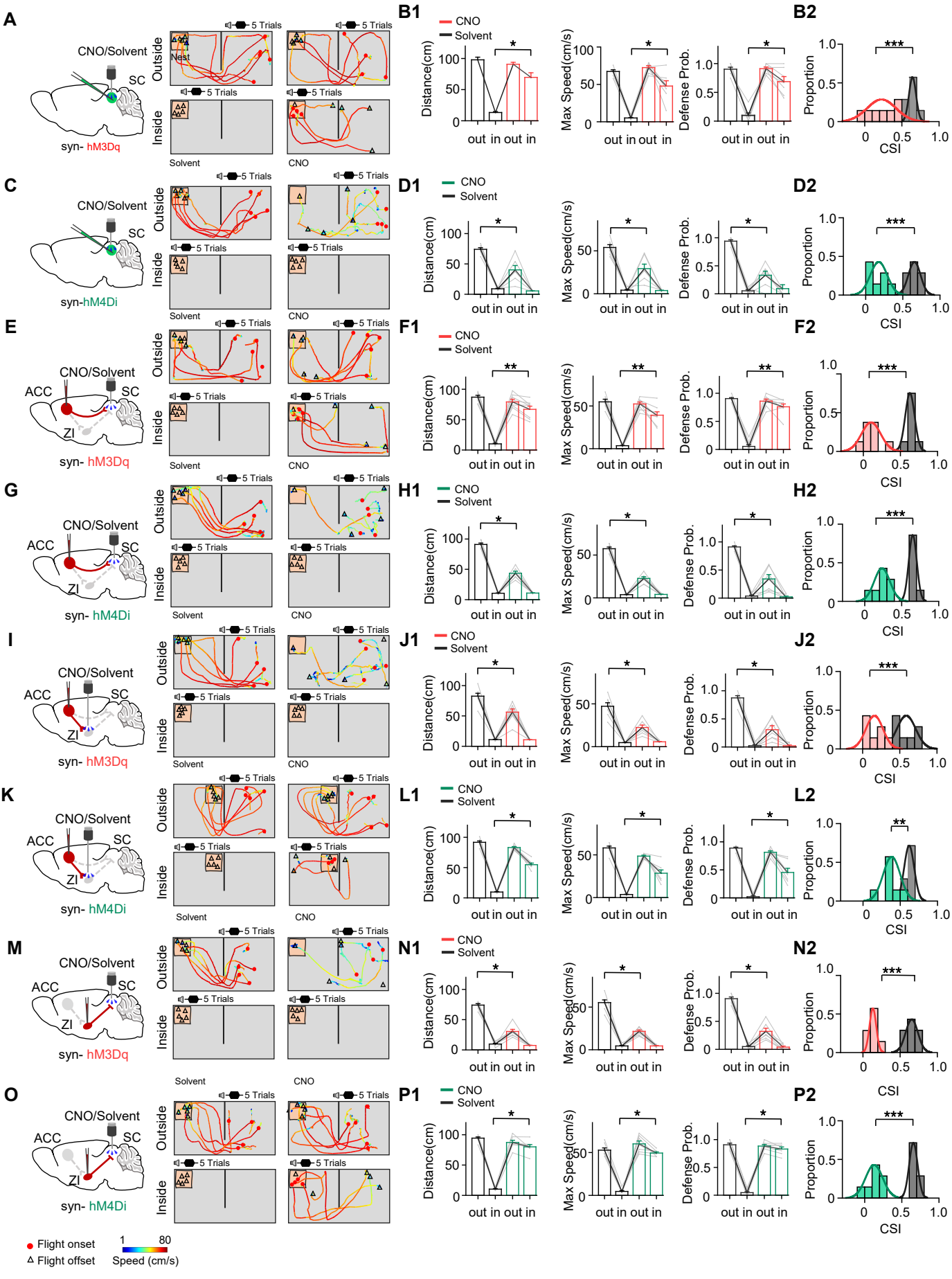
A
CNO/Solvent
SC
syn- hM3Dq
Outside
Inside
Nest
5 Trials
Solvent
CNO
B1
CNO
Solvent
Distance(cm)
Max Speed(cm/s)
Defense Prob.
out in out in
B2
Proportion
CSI
C
syn-hM4Di
D1
D2
E
ACC
ZI
F1
F2
G
H1
H2
I
J1
J2
K
L1
L2
M
N1
N2
O
P1
P2
Flight onset
Flight offset
1
80
Speed (cm/s)

Figure S6. Detailed experimental results for chemogenetic manipulations of ACC→SC and ACC→ZI→SC pathways. Related to figure 6.

(**A**) Left, schematic of chemogenetic activation of SC. Middle and right, trajectory-speed map for an example mouse under two scenarios (top, outside-nest bouts; bottom, inside-nest bouts) with solvent (middle) or CNO (right) infusion in SC.

(**B1**) Comparison of the total flight distance (left), maximum speed (middle) and defense probability (right) under two scenarios between solvent and CNO groups, respectively. Wilcoxon signed rank test (for distance, *P = 0.016, W = 28.00; for max. speed, *P = 0.016, W = 28.00; for flight probability, *P = 0.016, W = 28.00).

(**B2**) Distribution of CSIs without (grey) and with (color) chemogenetic activation. Kolmogorov-Smirnov test (***P < 0.001, D = 1.00), n = 7 mice.

(**C**-**D**) Similar to (**A**-**B**), but for chemogenetic inhibition of SC. (**D1**) Wilcoxon signed rank test (for distance, *P = 0.016, W = 28.00; for max speed, *P = 0.031, W= 27.00; for flight probability, *P = 0.016, W = 28.00). (**D2**) Kolmogorov-Smirnov test (***P < 0.001, D = 1.00), n = 7 mice.

(**E**) Left, schematic of chemogenetic activation of ACC glutamatergic axon terminals in the SC. Middle and right, trajectory-speed map for an example mouse under two scenarios (top, outside-nest bouts; bottom, inside-nest bouts) with solvent (middle) or CNO (right) infusion in SC.

(**F1**) Comparison of the total flight distance (left), maximum speed (middle) and defense probability (right) under two scenarios between solvent and CNO groups, respectively. Wilcoxon signed rank test (for distance, **P = 0.008, W = 36.00; for max. speed, **P = 0.008, W = 36.00; for flight probability, **P = 0.008, W = 36.00), n = 8 mice.

(**F2**) Distribution of CSIs without (grey) and with (color) chemogenetic activation. Kolmogorov-Smirnov test (***P < 0.001, D =1.00), n = 8 mice.

(**G**-**H**) Similar to (**E**-**F**), but for chemogenetic inhibition of ACC axon terminals in SC. (**G1**) Wilcoxon signed rank test (for distance, *P = 0.016, W= 28.00; for max. speed, *P = 0.016, W = 28.00; for flight probability, *P = 0.016, W = 28.00), n = 7 mice. (**G2**) Kolmogorov-Smirnov test (***P < 0.001, D = 1.00), n = 7 mice.

(**I**-**J**) Similar to (**E**-**F**), but for chemogenetic activation of ACC axon terminals in ZI. (**J1**) Wilcoxon signed rank test (for distance, *P = 0.031, W = 27.00; for max. speed, *P = 0.016, W = 28.00; for flight probability, *P = 0.016, W = 28.00), n = 7 mice. (**J2**) Kolmogorov-Smirnov test (***P < 0.001, D = 1.00), n = 7 mice.

(**K**-**L**) Similar to (**I**-**J**), but for chemogenetic inhibition of ACC axon terminals in ZI. (**L1**) Wilcoxon signed rank test (for distance, *P = 0.016, W = 28.00; for max. speed, *P = 0.016, W = 28.00; for flight probability, *P = 0.016, W = 28.00), n = 7 mice. (**L2**) Kolmogorov-Smirnov test (**P = 0.008, D = 0.86), n = 7 mice.

(**M**-**N**) Chemogenetic activation of ZI axon terminals in SC. (**N1**) Wilcoxon signed rank test (for distance, *P = 0.016, W= 28.00; for max. speed, *P = 0.016, W= 28.00; for flight probability, *P = 0.016, W= 28.00), n = 7 mice. (**N2**) Kolmogorov-Smirnov test (***P < 0.001, D = 1.00), n = 7 mice.

(**O**-**P**) Chemogenetic inhibition of ZI axon terminals in SC. (**P1**) Wilcoxon signed rank test (for distance, *P = 0.016, W= 28.00; for max speed, *P = 0.016, W = 28.00; for flight probability, *P = 0.016, W = 28.00,), n = 7 mice. (**P2**) Kolmogorov-Smirnov test (***P < 0.001, D = 1.00), n = 7 mice.

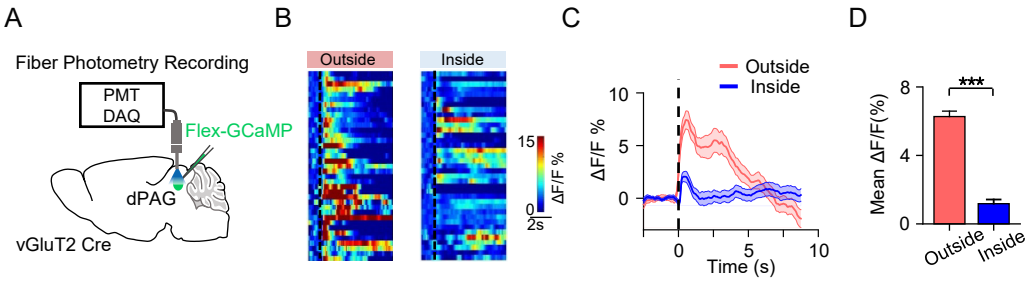

Figure S7. Fiber photometry recording of dPAG activity under two scenarios. Related to Figure 7.

(**A**) Schematic of fiber photometry recording of vGlu2^{+} neurons in dPAG.

(**B**-**C**) Heat maps (**B**) and average traces (**C**) of Ca^{2+} responses under two scenarios, aligned to the flight onset (outside-nest bouts) or noise onset (inside-nest bouts).

(**D**) Mean ΔF/F during 0–3 sec window after the flight onset (outside nest bouts) or noise onset (inside nest bouts). Wilcoxon signed rank test (***P < 0.001, W = 656.00), n = 37 bouts.